

Contents lists available at [SciVerse ScienceDirect](http://www.sciencedirect.com)

Organic Geochemistry

journal homepage: www.elsevier.com/locate/orggeochem

Contribution to characterisation of biochar to estimate the labile fraction of carbon

R. Calvelo Pereira^{a,*}, J. Kaal^b, M. Camps Arbestain^a, R. Pardo Lorenzo^c, W. Aitkenhead^a, M. Hedley^a, F. Macías^c, J. Hindmarsh^d, J.A. Maciá-Agulló^e^a New Zealand Biochar Research Centre, Private Bag 11222, Massey University, Palmerston North 4442, New Zealand^b Instituto de Ciencias del Patrimonio (Incipit), Consejo Superior de Investigaciones Científicas (CSIC), Rúa San Roque 2, 15704 Santiago de Compostela, Spain^c Departamento Edafología y Química Agrícola, Facultad de Biología, Universidad de Santiago de Compostela, 15782 Santiago, Spain^d Institute of Food, Nutrition and Human Health, Massey University, Palmerston North 4442, New Zealand^e Instituto Nacional del Carbón (CSIC), PO Box 73, 33080 Oviedo, Spain

ARTICLE INFO

Article history:

Received 24 May 2011

Received in revised form 5 September 2011

Accepted 7 September 2011

Available online xxxxx

ABSTRACT

Different analytical techniques were used to find the most reliable and economic method for determining the labile fraction of C in biochar. Biochar was produced from pine, poplar and willow (PI, PO and WI, respectively) at two temperatures (400 and 550 °C) and characterised using spectroscopic techniques [solid state ¹³C nuclear magnetic resonance spectroscopy (NMR)], molecular markers [pyrolysis–gas chromatography–mass spectrometry (Py–GC–MS)], thermogravimetry (TG), elemental composition and wet oxidation (potassium permanganate and potassium dichromate). Short term incubation (110 h) of an A horizon from an Umbrisol amended with the biochar samples at two doses (7.5 and 15 t ha⁻¹) was also carried out to provide supplementary information on the influence of biochar–soil interaction on CO₂ evolution. Spectroscopic analysis demonstrated that the degree of biochar carbonisation was influenced by the type of feedstock and heating conditions and followed the order WI-400 < PI-400 ~ WI-550 ~ PO-400 < PO-550 < PI-550. The thermo-labile fraction of the biochar samples, estimated from TG, ranged between 21% and 49%. The fraction of total C oxidised with potassium permanganate ($C_{\text{per}}/C_{\text{total}}$) was <50 g kg⁻¹ in all cases, whereas potassium dichromate ($C_{\text{dichro}}/C_{\text{total}}$) oxidation efficiency ranged between 180 and 545 g kg⁻¹. For each type of feedstock, the highest values of either chemically or thermally degradable C corresponded to the biochar produced at low temperature. Results indicate that low cost methodologies, such as dichromate oxidation and TG, reflected the degree of biochar carbonisation, and could therefore be used to estimate the labile fraction of C in biochar.

© 2011 Elsevier Ltd. All rights reserved.

1. Introduction

Biochar is pyrolysed organic material intended for use as a soil amendment to sustainably sequester C and concurrently improve soil function, while avoiding any adverse effects, on both the short and long terms (Lehmann and Joseph, 2009; Verheijen et al., 2009). Because of its condensed aromatic nature – especially when pyrolysed at high temperature – biochar is difficult for microorganisms to degrade and is therefore more stable than non-charred biomass (Paris et al., 2005; Lehmann et al., 2009; Shackley and Sohi, 2010), even though it is, over long periods, thermodynamically unstable under the oxidative conditions in most surface soils (Macías and Camps Arbestain, 2010). The relative stability of biochar determines the length of its contribution to the mitigation of greenhouse gas (GHG) emissions. However, its properties, including stability, depend not only on feedstock type and processing conditions (referred to as intrinsic recalcitrance) (Labbe et al., 2006;

Nguyen and Lehmann, 2009), but also on the pedoclimatic conditions of the soil to which it was applied (Czimeczik and Masiello, 2007).

Obviously, if biochar is to become accountable in trading C offset, robust protocols are needed to demonstrate and monitor its stability over time in the environment where it is deployed (Lehmann et al., 2009). In the context of biochar as C storage tool for mitigating GHG emissions and, based on the 100 yr time horizon used to calculate the global warming potential, as in the Kyoto Protocol (Forster et al., 2007), any amount of C stored from the atmosphere for at least 100 yr could be computed as a GHG mitigation benefit. Unfortunately, direct measurements in a timeframe of a century or longer make the approach unattainable. The stability of biochar should thus be evaluated in terms of the labile and stable fraction of C in the charred material (Lehmann et al., 2006, 2009; Hammes and Schmidt, 2009), the first being the fraction decomposed or lost with a turnover time ranging between weeks and decades, the second being the amount remaining in the soil C pool for centuries and millennia. While the mean residence time of the stable fraction might be difficult to determine, knowledge of

* Corresponding author. Tel.: +64 6 356 9099; fax: +64 6 350 5632.

E-mail address: R.Calvelopereira@massey.ac.nz (R. Calvelo Pereira).

Table 1
Total C, N and ash content (g kg^{-1}) of pine, poplar and willow feedstock, proportion of cellulose, hemicellulose, lignin and neutral detergent fibre (NDF), and heating rate and highest temperature.

Sample	C (g kg^{-1})	N (g kg^{-1})	Ash (g kg^{-1})	Cellulose (%)	Hemicellulose (%)	Lignin (%)	NDF (%)	HR ^a	
								400 °C	550 °C
Pine	487	1.9	10	38.9	16.1	29.1	84.1	38	24
Poplar	479	4.6	22	45.4	15.1	23.0	83.5	36	48
Willow	476	9.2	57	37.4	14.8	23.4	75.5	62	46

^a Heating rate, °C min⁻¹.

Table 2
Characteristics of biochar from pine, poplar and willow at highest heating temperature.

Biochar	Feedstock	Temp. (°C)	pH	Yield (%)	C (g kg^{-1})	N (g kg^{-1})	H (g kg^{-1})	O (g kg^{-1})	Ash ^a (g kg^{-1})	IC ^b (g kg^{-1})	Recovery (%)		Atomic ratio		S _{BET} ^d ($\text{m}^2 \text{g}^{-1}$)
											C	N	O/C	H/C	
PI-400	Pine	400	6.9	34.9	767	6	46	145	37	<d.l. ^c	54.9	100.6	0.14	0.71	1
PO-400	Poplar		7.2	29.7	755	10	42	152	40	<d.l. ^c	46.9	66.2	0.15	0.66	3
WI-400	Willow		7.5	37.8	662	15	35	231	57	2.7	52.6	59.3	0.26	0.63	3
PI-550	Pine	550	7.9	28.4	847	6	35	71	41	<d.l. ^c	49.3	87.6	0.06	0.50	368
PO-550	Poplar		8.8	26.9	758	11	36	130	65	2.2	42.6	64.5	0.13	0.56	55
WI-550	Willow		8.6	28.8	791	17	35	82	75	2.3	47.8	52.9	0.08	0.52	149

^a At 900 °C.

^b IC/C_{total}, inorganic C (CO₂-C).

^c < Detection limit.

^d Specific surface area.

the labile fraction under different pedoclimatic conditions should provide valuable information for future assessments of the proportion of stable C in biochar needed for trading C offset.

Recent studies that have focussed on characterisation of charred material – from which the labile fraction of C can be estimated – typically rely on the use of one of the following: (i) spectroscopic approaches, such as solid state nuclear magnetic resonance spectroscopy (solid state ¹³C NMR) (McBeath and Smernik, 2009) and Fourier transform infrared spectroscopy (FTIR) (Michel et al., 2009); (ii) thermal analysis (thermogravimetry, TG; de la Rosa et al., 2008); (iii) molecular markers by means of pyrolysis–gas chromatography–mass spectrometry (Py–GC–MS; Kaal et al., 2008a, 2009) or the benzene polycarboxylic acid method (Brodowski et al., 2005); (iv) an array of chemo-thermal (Hammes et al., 2007) and chemical (e.g. potassium dichromate: Knicker et al., 2007; nitric acid: Marques Trompowsky et al., 2005) oxidation. Studies to determine the labile fraction of C in biochar under specific pedoclimatic conditions include incubation experiments based on CO₂ efflux (Kimetu and Lehmann, 2010; Bruun et al., 2011) and C isotope evolution (Bruun et al., 2008; Kuzyakov et al., 2009; Zimmerman et al., 2011). To our knowledge, however, no specific attempts have been made to look at relationships among the different estimates of the labile fraction of C in biochar.

The objectives of this study were (i) to characterise the C fraction in biochar produced from different feedstock types (pine, poplar and willow) at two temperatures (400 and 550 °C) using Py–GC–MS and solid state ¹³C NMR, and (ii) to compare the results with those from less sophisticated but more affordable techniques (TG, oxidation with different reagents) to find the most reliable and economic method for determining the intrinsic labile fraction of C in biochar. In addition, short term incubation using an acid soil with and without the addition of these biochar samples was carried out. These were not designed to address specifically the short term lability of C in biochar, as isotopes were not used, but rather to provide supplementary information on the influence of biochar–soil interaction on CO₂ evolution.

2. Material and methods

2.1. Feedstock and biochar

Pinus radiata wood chips (pine; PI), *Populus nigra 'Italica'* (poplar; PO) and *Salix matsudana* var. *pendula* prunings (willow; WI) were used as feedstock. The pine and willow originated from mature stands, whereas the poplar prunings were from a 1 yr old plantation. The material was chipped with a commercial chipper to 3 mm to 4 cm particle size. The particle size was heterogeneous for the three feedstocks. The cellulose, hemicellulose and lignin contents were determined using the Fibertec System M (Tecator, Hoganas, Sweden). The method is based on sequential treatment with neutral detergent, acid detergent, 72% H₂SO₄ and ashing (Robertson and Van Soest, 1981). The neutral detergent step washes out the cellular content and ash; the residual fraction is referred to as neutral detergent fibre (NDF). This residue is further fractionated. With the acid detergent treatment of NDF, cell walls are broken down and the residual fraction is referred to as acid detergent fibre (ADF). Hemicellulose is estimated as NDF–ADF. With a subsequent H₂SO₄ treatment, cell walls are digested and an acid detergent lignin (ADL) residue is obtained. Cellulose is estimated as ADF–ADL and ADL is assumed to be mostly lignin, although it may also contain suberin and cutin from bark remains.

Biochar was produced using a self-purged, gas-fired, stainless steel rotating drum kiln (5 l). The kiln, designed to study pyrolysis at a laboratory scale, is located at Massey University. The feedstock samples were dried overnight in an oven at 65 °C. Aliquots (200 g) of PI, PO and WI were pyrolysed at 400 °C or 550 °C in the kiln, which was rotated at 0.17 Hz to ensure even heating and mixing. The gas produced was collected via an exhaust vent and a condenser system. When the desired temperature was reached, the heating source was switched off and the kiln was allowed to cool to room temperature. To prevent oxygen entering the system during the cooling phase, gas that had been expelled from the drum was collected and fed back in through the exhaust. Full control of

Table 3

Carbon lability for biochar produced from pine, poplar and willow at highest heating temperature (for definition of variables see text).

Biochar	Temp. (°C)	C _{thermo} (%)	C _{fixed} (g kg ⁻¹)	C _{dichro} /C _{total} (g kg ⁻¹)	C _{per} /C _{total} (g kg ⁻¹)
PI-400	400	38	574	318	41
PO-400		35	609	393	39
WI-400		49	460	545	46
PI-550	550	21	727	180	9
PO-550		28	658	307	18
WI-550		40	527	323	5

the heating rate was not possible, but temperature changes were monitored and mean heating rates are reported in Table 1.

2.2. Biochar characterisation

Biochar samples were characterised using different analytical techniques that differed in (i) the type of information provided (qualitative vs. quantitative), (ii) the different properties they rely on (thermal degradability vs. chemical “oxidisability”) and (iii) ease of use and cost.

2.2.1. Elemental analysis

Total C (C_{total}), H and N contents were determined using a Tru-Spec CHNS analyser (LECO Corp. St. Joseph, MI). The ash content was determined by way of thermal analysis using a TG analyser (SDT Q600, TA Instruments, Melbourne, Australia). The samples (both feedstock and biochar; 5–15 mg) were placed in an Al₂O₃ crucible and heated from room temperature to 900 °C (at 5 °C min⁻¹) under a N₂ atmosphere; weight loss (in wt.%) and weight loss rate (in wt.% °C⁻¹) were recorded continuously; thereafter, an air current was provided and the ash was determined when there was no further weight change (method modified after Sevilla and Fuertes (2010)). Oxygen was estimated as follows: O = 100 – (C + H + N + ash) (all wt.%). The inorganic C (IC) content (i.e. CO₃²⁻) was determined by measuring the weight loss associated with the endothermic peak at ca. 600–700 °C (Vassileva and Vassilev, 2005). As values were <0.3% of total C (Table 2), total C was assumed to be all organic and is reported as C_{total}.

2.2.2. TG analysis

Thermogravimetric TG and derivative (DTG) curves were obtained using the SDT Q600 instrument described above. The TG and DTG signals were exported to the TA Universal Analysis Software for further analysis. The weight loss between 110 and 900 °C in a N₂ atmosphere was considered as the biochar volatile matter content, whereas the loss of weight at 900 °C after the introduction of air current was considered as the stable, thermo-resistant fraction or fixed C (C_{fixed}). The fraction of volatile matter with respect to the sum of volatile matter content and fixed C is considered as the thermo-degradable fraction of biochar (C_{thermo}, ash-free, dry basis; expressed as %, see Table 3).

2.2.3. Py-GC-MS

Pt filament coil probe Py-GC-MS was performed with a Pyroprobe 5000 (Chemical Data Systems, Oxford, USA) coupled to a 6890N GC and 5975B MSD GC-MS system (Agilent Technologies, Palo Alto, USA). Finely ground samples (ca. 1 mg) of both feedstock type and biochar were embedded in fire-polished quartz tubes that contained glass wool. The samples were pyrolysed at 750 °C for 10 s (10 °C ms⁻¹, conditions found to be suitable for charred material; Kaal et al., 2009; Kaal and Rumpel, 2009). The interface and the GC inlet (splitless mode) were at 325 °C. The GC oven was heated from 50 to 320 °C (held 5 min) at 20 °C min⁻¹. The GC-MS transfer line was at 325 °C, the ion source (electron ionisation mode, 70 eV) at 230 °C and the quadrupole detector at 150 °C; scan range was *m/z* 45–500. The GC instrument was equipped with a

(non-polar) HP-5MS 5% phenyl, 95% dimethylpolysiloxane column (ca. 30 m × 0.25 mm i.d.; film thickness 0.25 μm). He was the carrier gas (1 ml min⁻¹). Compounds were assigned using the NIST '05 library and Py-GC-MS literature for cellulose, lignin, wood and black carbon (BC; Faix et al., 1987; Pouwels et al., 1989; Pastorova et al., 1994; Schnitzer et al., 2007; de la Rosa et al., 2008; Kaal et al., 2009; Song and Peng, 2010). Of the pyrolysis products, 25 were quantified using the peak area of their characteristic fragment ions (Table 4). This semi-quantitative dataset provides relative contributions of the pyrolysis products expressed as a proportion (%) of total quantified peak area (TQPA), which allows a more detailed comparison between samples than from visual inspection of pyrograms alone.

2.2.4. Solid state CPMAS ¹³C NMR spectroscopy

Solid state ¹³C CPMAS (cross polarisation, magic-angle spinning) NMR spectra were obtained at a ¹³C frequency of 50.3 MHz with a Bruker AMX 200 MHz spectrometer (Rheinstetten, Germany; Hina et al., 2010). Samples were packed in a cylindrical zirconia rotor (7 mm diam.) with Kel-F end caps and spun at 4500 ± 200 Hz in a Doty Scientific MAS probe. Free induction decays were acquired with a 1 H 90° pulse of 5.5 μs and a sweep width of 40 kHz; 1216 data points were collected over an acquisition time of 15 ms, a cross polarisation contact time of 1000 ms and a relaxation time of 3 s; 4000 scans were acquired. The spectra were zero filled to 8192 data points and processed with 100 Hz Lorentzian line broadening and 0.005 s Gaussian broadening. Chemical shifts were externally referenced to the ¹³C resonance of glycine. It must be acknowledged that CPMAS ¹³C NMR spectroscopy often under-detects aromatic C and an unequivocal quantification is not feasible (Smernik et al., 2002).

2.2.5. Chemical oxidation

Two reagents were used to assess the labile fraction of C in biochar samples: potassium dichromate and potassium permanganate. The organic C oxidised with potassium dichromate (C_{dichro}) was obtained following the Walkley-Black method as modified by Wolbach and Anders (1989) and Knicker et al. (2007). Results are expressed as the fraction of total C oxidised by potassium dichromate (C_{dichro}/C_{total}). Organic C oxidised with potassium permanganate (C_{per}) was determined following the methodology of Tirol-Padre and Ladha (2004). Results were expressed as the fraction of total C oxidised by potassium permanganate (C_{per}/C_{total}).

2.2.6. Other analyses

Biochar pH was measured using a 1% (wt./wt.) suspension of biochar in deionised water (Ahmedna et al., 1997). The suspension was heated in a water bath to ca. 90 °C and stirred for 20 min to allow dissolution of the soluble components. After cooling to room temperature, the pH of the suspension was determined with a combined pH electrode (PHM83, Radiometer, Copenhagen). N₂ adsorption analysis for specific surface area (Brunauer et al., 1938) was performed using a Micromeritics ASAP 2020 volumetric adsorption system. Values of the Brunauer, Emmett and Teller equation (BET) surface area, S_{BET}, are reported in Table 2. Samples were previously outgassed at 250 °C for 4 h.

Table 4
Py–GC–MS products, fragment ions for quantification, tentative biocomponent assignment (group) and relative contribution for feedstock type (FS) and biochar samples.

n	Product	Group	t_R^a	m/z	Pine			Poplar			Willow		
					FS	400 °C	550 °C	FS	400 °C	550 °C	FS	400 °C	550 °C
1	Benzene	BTX ^b	1.782	78	0.5	1.5	21.9	0.7	2.3	18.4	0.9	1.3	16.4
2	Toluene	BTX	2.306	91 + 92	1.9	8.7	31.7	2.9	18.1	57.9	5.3	21.6	58.0
3	3/2-Furaldehyde	Carbohydrate	2.759	95 + 96	6.6	0.8	0.0	4.6	0.3	0.0	7.0	1.8	1.1
4	C ₂ -benzene (3 isomers)	BTX	2.9–3.3	91 + 106	1.1	4.8	6.7	1.2	8.5	6.7	1.6	3.1	11.4
5	Phenol	Lignin	3.781	94 + 66	4.0	10.2	7.9	8.2	17.4	3.9	9.5	13.3	2.6
6	Benzonitrile	N compounds	3.947	103 + 76	0.0	0.1	2.0	0.0	0.2	1.1	0.0	0.2	0.8
7	Benzofuran	Carbohydrate	4.002	118 + 89	0.3	0.8	1.8	0.4	1.4	1.6	0.0	0.9	1.9
8	C ₁ -phenol (2 isomers)	Lignin	4.2–4.6	107 + 108	6.7	18.1	2.2	5.2	23.6	2.2	5.8	12.2	1.7
9	Guaiacol	Lignin	4.641	109 + 124	6.0	14.4	0.0	4.2	4.2	0.0	2.6	10.8	0.0
10	C ₂ -Phenol (3 isomers)	Lignin	4.9–5.3	107 + 122	4.1	10.6	0.5	2.9	13.0	0.6	2.4	6.0	0.5
11	4-Methylguaiacol	Lignin	5.411	123 + 138	5.8	15.1	0.0	3.8	2.7	0.0	2.3	7.0	0.0
12	Catechol	Other	5.495	110 + 64	10.5	6.2	1.0	7.6	2.4	0.2	4.8	2.0	0.1
13	Naphthalene	PAH ^c	5.518	128	0.1	0.3	15.2	0.1	0.6	3.7	0.1	0.3	2.5
14	C ₁ Naphthalene (2 isomers)	PAH	6.1–6.4	142 + 115	0.1	0.9	3.2	0.2	1.5	1.9	0.3	0.7	1.5
15	4-Vinylguaiacol	Lignin	6.287	135 + 150	12.5	3.5	0.0	8.3	0.6	0.0	6.0	1.7	0.2
16	Syringol	Lignin	6.544	154 + 139	0.0	0.0	0.0	4.4	1.0	0.0	3.0	4.0	0.0
17	Propenylguaiacol (3 isomers)	Lignin	6.9–7.3	164 + 149	6.1	1.0	0.0	3.8	0.2	0.0	3.0	0.5	0.0
18	4-Methylsyringol	Lignin	7.188	168 + 153	0.0	0.0	0.0	3.4	0.7	0.0	2.3	4.3	0.0
19	Dibenzofuran	Carbohydrate	7.837	168 + 139	0.0	0.2	4.1	0.0	0.3	1.2	0.0	0.1	0.6
20	4-Vinylsyringol	Lignin	7.917	180 + 165	0.0	0.0	0.0	5.9	0.2	0.0	6.3	1.2	0.0
21	Propenylsyringol (3 isomers)	Lignin	8.4–8.7	194 + 179	0.0	0.0	0.0	3.7	0.1	0.0	4.3	0.3	0.0
22	Levogluconan	Carbohydrate	8.593	60 + 73	33.4	2.6	0.0	28.1	0.4	0.0	31.5	4.8	0.0
23	Diketodipyrrole	N compounds	8.866	186 + 93	0.1	0.1	0.0	0.1	0.2	0.0	0.5	1.6	0.1
24	Phenanthrene/anthracene	PAH	9.420	178	0.0	0.1	2.0	0.0	0.1	0.5	0.0	0.1	0.4
25	C ₁₆ -fatty acid	Other	9.972	60 + 73	0.2	0.2	0.0	0.4	0.1	0.0	0.5	0.3	0.1

^a Retention time, min.^b Benzene, toluene, ethylbenzene, styrene and xylenes.^c Polycyclic aromatic hydrocarbon.**Table 5**
Main properties of soil used in incubation experiments.

Soil	Depth (cm)	pH _{H2O}	pH _{KCl}	C ^a (g kg ⁻¹)	OC ^b (g kg ⁻¹)	C _p ^c (g kg ⁻¹)	N ^a (g kg ⁻¹)	C/N	Exchange complex (cmol(+) kg soil ⁻¹)					
									Ca ²⁺	Mg ²⁺	Na ⁺	K ⁺	Al ³⁺	H ⁺
Umbrisol (UM)	0–40	4.9	4.3	59.4	56.1	18.2	0.4	19.9	0.15	0.07	0.56	0.15	3.92	–

^a Total C, analysed using LECO.^b Total organic C, oxidised with acid dichromate oxidation.^c Organic C oxidised with sodium pyrophosphate.

2.3. Short term mineralisation

A fresh soil sample from the A horizon (0–40 cm depth) of an Haplic Umbrisol (UM) developed on gneiss from Campaño (Galicia, NW Spain) was used to study the short term CO₂ evolution of soil samples amended with the biochar samples vs. unamended soil. The soil was under eucalyptus (*Eucalyptus globulus* Labill.) stands at the time of sampling. It was wet sieved through 2 mm and stored at 4 °C. The main chemical characteristics are reported in Table 5. Fresh samples equivalent to 10 g air-dried soil were mixed with the biochar and placed in incubation jars. Two application rates of biochar were considered: 5 and 10 g kg⁻¹, which corresponded to doses of ca. 7.5 and 15 t ha⁻¹ respectively under field conditions, assuming 15 cm depth and a soil bulk density of 1 kg dm⁻³. The soil without biochar amendment was used as a control. All samples were pre-incubated overnight before starting the experiment. A nutrient solution was added to the jars to maintain biological activity during the experiment. This solution consisted of 60 g (NH₄)₂SO₄ and 6 g KH₂PO₄ diluted in 1 l distilled water (Zimmerman, 2010). The moisture content of the soil and mixtures was adjusted to the field capacity of the soil without biochar amendment (gravimetric moisture content of 37%). Incubation was at 25 °C during 110 h, in triplicate. The basal respiration of biochar mixtures was measured with a Micro-Oxymax Respirometer (Columbus Instruments, Columbus, OH).

3. Results

3.1. Properties of feedstock and process conditions during pyrolysis

Feedstock C content was 487, 479 and 476 g kg⁻¹ for pine, poplar and willow, respectively (Table 1). N content was low, varying between 1.9 (pine) and 9.2 g kg⁻¹ (willow; see Table 1). The cellulose, hemicellulose and lignin contents of feedstock types are summarised in Table 1. The highest cellulose content (45%) was in the poplar prunings and the highest lignin content in the pine wood (29%). The recorded heating rate was variable, ranging between 24 °C min⁻¹ for pine (at a maximum heating temperature of 550 °C) and 62 °C min⁻¹ for willow (at a maximum heating temperature of 400 °C; Table 1).

3.2. Properties of carbonised material

The pH values of the biochar ranged from 6.9 in PI-400 to 8.8 in PO-550 (Table 2). Biochar produced at 550 °C (pH 7.9–8.8) had a higher pH than biochar produced at 400 °C (pH 6.9–7.5). Biochar yield, defined as the mass ratio of biochar recovered after pyrolysis and the initial feedstock, is reported in Table 2; values for biochar produced at 400 °C ranged from 29% to 38%, whereas values at higher temperature were smaller and less variable between feedstock types, ranging from 27% to 29% (Table 2).

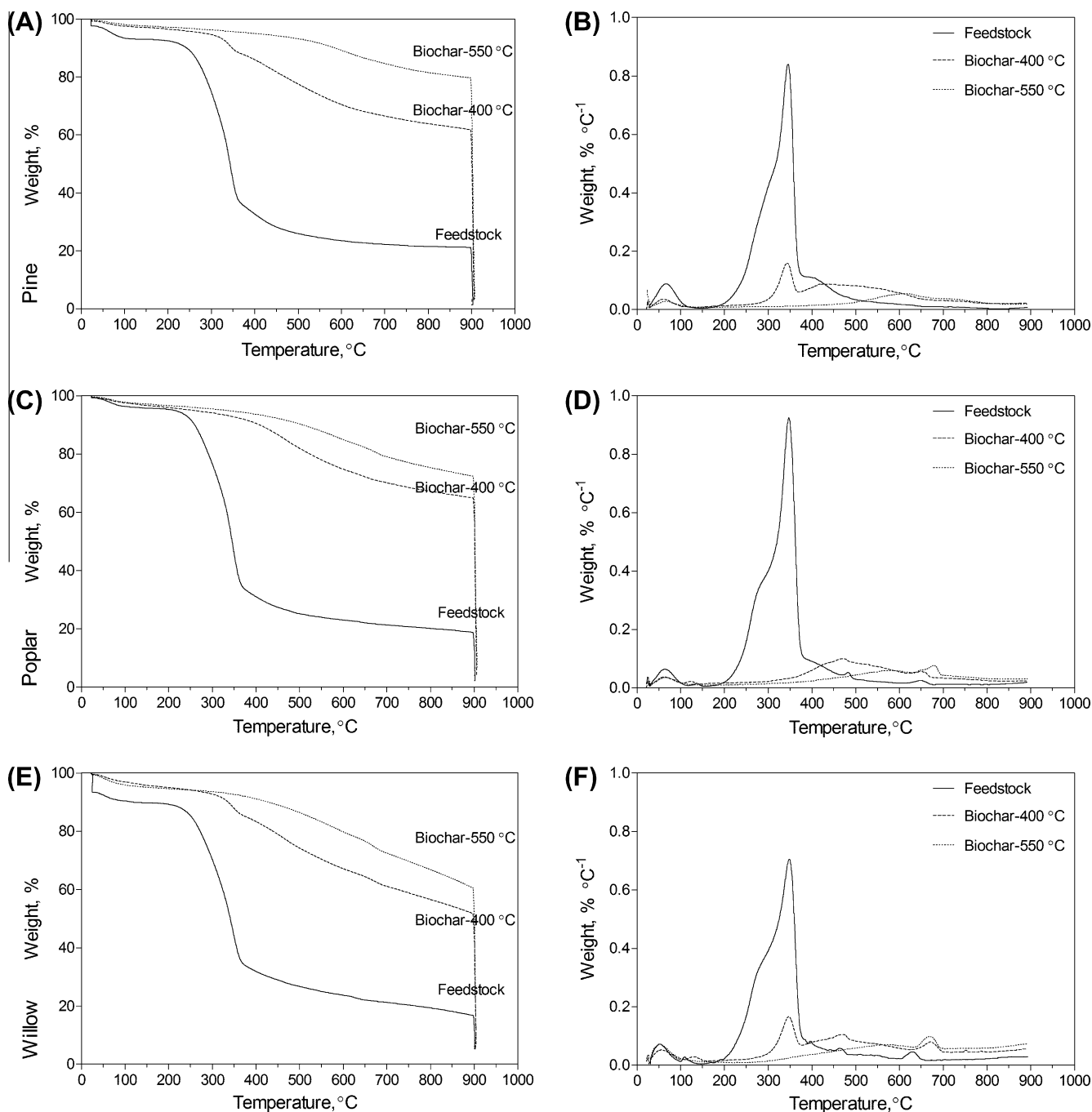


Fig. 1. TG and DTG curves for feedstock and biochar samples (highest heating temperatures 400 and 550 °C): (A and B) pine; (C and D) poplar; (E and F) willow.

Biochar C content was high, ranging from 662 g kg⁻¹ for WI-400 to 847 g kg⁻¹ for PI-550 (Table 2). Recovered C, defined as the proportion of the original C retained in the carbonised sample, ranged between 47% and 55% in the 400 °C biochar and between 43% and 49% in the 550 °C biochar (Table 2). The N content was low, as expected for biochar from woody material. However, upon charring, N enrichment relative to the original feedstock was observed. A high recovery of N was specifically evident for the lower N content char samples, PI-400 and PI-550 (100% and 88%, respectively; Table 2), although the low N content of the wood increased the uncertainty in these estimates. The elemental concentrations of H and O were always higher in the 400 °C biochar than the 550 °C biochar; this resulted in lower H/C and O/C atomic ratio val-

ues at increasing final temperature (Table 2). The H/C values followed the order PI > PO > WI for 400 °C biochar and PO > WI > PI for 550 °C biochar. Carbonate was found in WI-400, WI-550 and PO-550, where the IC content ranged between 2.2 and 2.7 g kg⁻¹; these samples were also those with the greatest ash content (Table 2). High temperature biochar (PI-550, PO-550 and WI-550) showed much greater surface area (S_{BET} 55–368 m² g⁻¹; Table 2) than the corresponding low temperature biochar (PI-400, PO-400 and WI-400; $S_{\text{BET}} < 5$ m² g⁻¹); the PI-550 sample had the greatest surface area (368 m² g⁻¹).

The results on the “oxidisability” of C in biochar indicated that $C_{\text{per}}/C_{\text{total}}$ values were <50 g kg⁻¹ for all biochar samples whereas those for $C_{\text{dichro}}/C_{\text{total}}$ ranged between 180 and 545 g kg⁻¹ (Table 3).

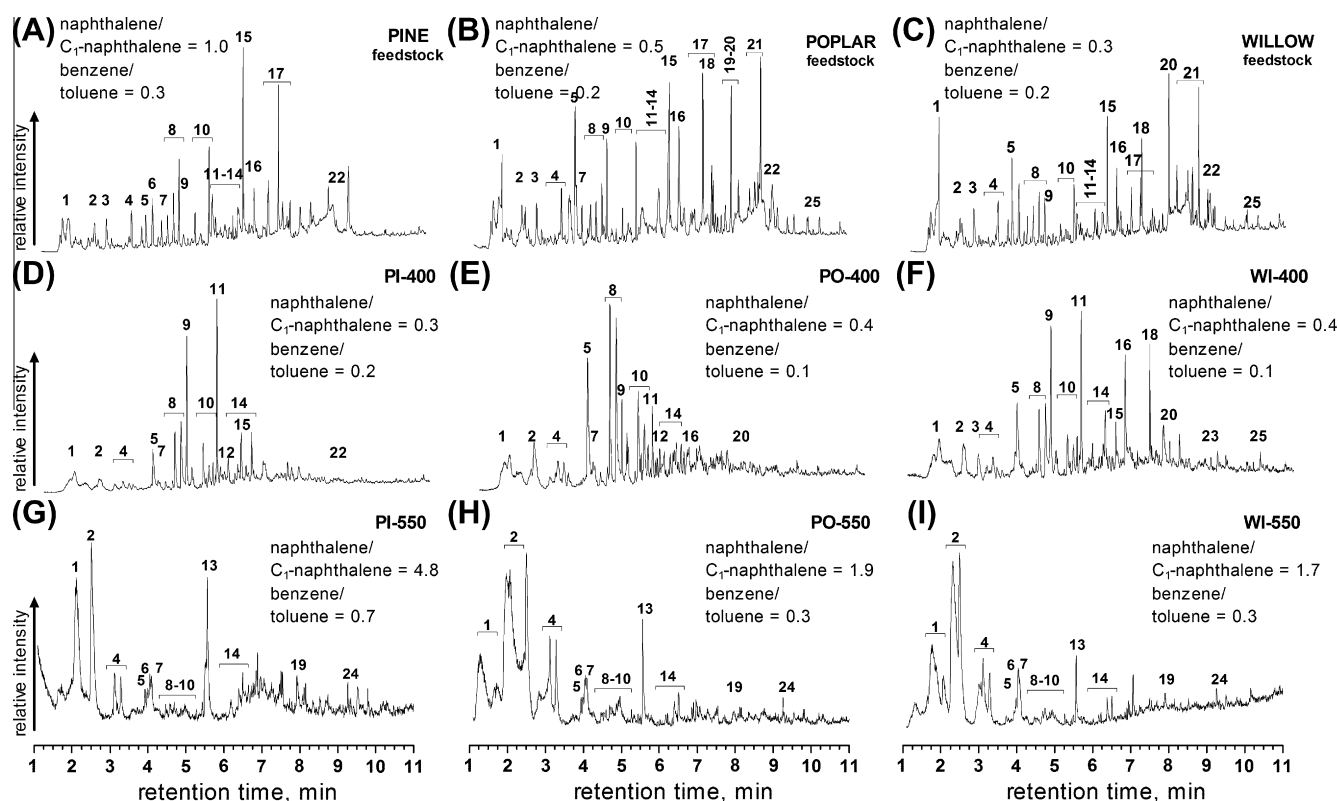


Fig. 2. Total ion current pyrograms of feedstock and biochar samples (highest heating temperature 400 and 550 °C). (A, D, and G) pine, (B, E, and H) poplar and (C, F, and I) willow. Numbers refer to pyrolysis products in Table 4. Ratios of pyrolysis products (naphthalene/C₁ naphthalene and benzene/toluene) are reported.

Irrespective of feedstock type, both reagents resulted in greater oxidation of low temperature biochar than high temperature biochar (Table 3).

3.3. Thermal analysis

The TG and DTG curves are shown in Fig. 1 and the data are summarised in Table 3. Differences in thermo-degradability among the feedstock and biochar samples were evident, although all samples displayed an initial mass loss up to about 110 °C, attributed to water loss, and a final steady decrease in weight above the peak temperature of heating (Fig. 1). The main changes were between 220 and 550 °C. As expected, biochar produced at 400 °C and 550 °C showed strong weight loss above 400 °C and 550 °C, respectively. Weight loss followed the order feedstock > biochar-400 > biochar-550 (Fig. 1). However, the curves also revealed that PI-400 and WI-400 had a peak in the DTG signal slightly below 400 °C. Finally, it should be noted that PO-550, WI-400 and WI-550 showed a small but clear peak on the DTG curve around 650 °C (Fig. 1), which was used to quantify the IC (C–CO₃) content.

3.4. Py–GC–MS

The feedstock samples and the 400 °C biochar samples produced good quality pyrograms; however, the 550 °C biochar samples gave very weak signals (Fig. 2; numbers in italics refer to major individual compounds cf. Table 4) because of high thermal stability and therefore limited the “pyrolysability” of large polyaromatic clusters. Therefore, the results from the high temperature biochar may be expected to represent only a small fraction of the sample. Nonetheless, the ratios of some products from the high temperature biochar can still provide information on charring intensity (Kaal and Rumpel, 2009).

3.4.1. Lignin derivatives

Feedstock samples produced many methoxyphenols (guaiacols and syringols, depending on wood type) on pyrolysis, which originate from lignin. Pine feedstock produced only methoxyphenols of the guaiacol type, dominated by 4-vinylguaiacol (15), C₃ guaiacols (17), 4-methylguaiacol (11) and other guaiacyl-based compounds such as vanillic aldehyde (Fig. 2A). Angiosperm wood contains syringyl lignin (with 2 methoxyls/aromatic ring), producing syringols upon pyrolysis. Hence, poplar feedstock produced (Fig. 2B) large peaks for 4-vinylguaiacol (15), 4-methylsyringol (18), 4-vinylsyringol (20) and C₃ syringols (21). Willow lignin produced more syringols than poplar, with 4-vinylsyringol (20) and C₃ syringols (21) giving the strongest signal (Fig. 2C). The very small proportion of N-containing products (see below), together with the relatively low N content of feedstock and the corresponding biochar measured from elemental analysis (Tables 1 and 2), indicate that polypeptides were negligible in the samples. Thus, phenols (5, 8, 10) probably originated largely from lignin as well, perhaps with a small contribution from carbohydrate-derived phenols (Pastorova et al., 1994).

The biochar fingerprints showed clear differences vs. the feedstock samples (Fig. 2D–I). PI-400 exhibited a strong decline in C₃ guaiacols (17) and 4-vinylguaiacol (15), and an increase in guaiacol (9) and 4-methylguaiacol (11), suggesting degradation of the alkyl side chains of the lignin monomers, which might correspond to depolymerisation of the lignin. The pyrogram of PI-550 showed no methoxyphenols and only some phenol (5) remained, reflecting virtually complete demethoxylation and profound dehydroxylation of lignin (Fig. 2G). In the case of PO-400, lignin degradation was more severe than in PI-400, as the methoxyphenols (both guaiacols, 9 and syringols, 16) decreased strongly and phenols (5, 8) were dominant. Phenols were negligible for PO-550, which is indicative of further degradation of lignin precursors (Fig. 2H;

Table 4). Of the biochar samples, WI-400 gave the largest peaks for guaiacol (9), 4-methylguaiacol (11), syringol (16) and 4-methylsyringol (18), suggesting that, although the C₃ side chain was largely degraded upon charring, the methoxylic and phenolic functional groups were largely intact (Fig 2F). Nonetheless, at 550 °C, these methoxyphenols could no longer be detected (Fig. 2I; Table 4).

3.4.2. Carbohydrate derivatives

Feedstock samples were dominated (ca. 30% of TQPA) by levoglucosan (22), the principal pyrolysis product of intact (uncharred) cellulose and hemicellulose polysaccharides. In addition, several furans and furaldehydes (from here on furans 3, 7, 19), cyclopentenones and pyrans – also originating from carbohydrates (Pouwels et al., 1989) – were detected from the feedstock samples. The proportion of levoglucosan (22) diminished on charring at 400 °C (2.5–5% for PI-400 and WI-400, and to trace proportions in PO-400). The 550 °C biochar samples produced only trace amounts of 3/2 furaldehyde (3), while benzofurans (7) and dibenzofurans (19) increased, probably reflecting carbohydrate aromatisation upon charring (see also Boon et al., 1994).

3.4.3. “BTX” (benzene, toluene, ethylbenzene, styrene, and xylenes)

These non-specific aromatic compounds may be produced after pyrolysis of almost any biomass source. Feedstock samples produced some BTX compounds (3–8% of TQPA), which may partially originate from artificially (i.e. during analytical pyrolysis) demethoxylated and dehydroxylated methoxyphenolic compounds (Kaal et al., 2009). A significant proportion of the benzenes and polynuclear aromatic hydrocarbons (PAHs; see below) may originate from charred carbohydrates as well (Boon et al., 1994; Pastorova et al., 1994). For biochar samples, the general trend in BTX proportion was similar for the three feedstock types (Fig. 2D–I). At 400 °C, the proportion of all BTX increased with respect to the feedstock (25–29% of TQPA). The proportion of BTX increased further for the 550 °C biochar (60–96% of TQPA). Of the BTX, toluene (2) and C₂ benzenes (4) were present in higher concentration than benzene (1) in the 400 °C biochar samples, whereas the opposite was true for the 550 °C biochar. PO-550 and WI-550 gave two peaks for benzene (1) as well as for toluene (2). Re-analysis of these samples with the pyrolysis step delayed for 5 min (with the sample in the pyrolysis-interface at 325 °C and the GC–MS system running) showed an initial pre-pyrolysis peak for these compounds. Thus, it is likely that one peak originated from evaporation of trapped aromatics while the other peak reflected a true pyrolysis product.

3.4.4. PAHs

Feedstock samples did not produce detectable levels of PAHs after the analytical pyrolysis, as expected (Rumpel et al., 2007). In the case of biochar, the PAH fingerprints after the second pyrolysis were similar (Fig. 2D–I; Table 4); small contributions of PAHs were detected for 400 °C biochar while they dominated the pyrolysates of the 550 °C biochar together with the BTX. The PAHs were naphthalene (13), alkyl naphthalenes (14), biphenyl, phenanthrene/anthracene (24; co-elution), fluorene, biphenyl and possibly pyrene (*m/z* 202 at the expected retention time). PI-400 produced several small peaks with mass spectral patterns that strongly resembled those of C₂ phenanthrenes (*m/z* 206 + 189), C₃ phenanthrenes (*m/z* 220 + 205) and retene (*m/z* 219 + 234; i.e. 1-methyl-7-isopropylphenanthrene, a C₄ phenanthrene), which were not detected in the pyrograms of pine feedstock, suggesting that they originate from charred (dehydrogenated) diterpenoids. Re-analysis of this sample with the pyrolysis step delayed did not allow elucidating whether these retene-like compounds were evaporation products trapped in biochar micropores or actual pyrolysis products of macromolecular structures. Values of benzene/toluene and naphthalene/C₁ naphthalene ratios increased 2-fold to 5-fold

and 4-fold to 14-fold respectively, from 400 °C biochar and 550 °C biochar (Fig. 2), suggesting elimination of alkyl cross linkages with increasing biochar production temperature.

3.4.5. N-containing products

As expected, the proportion of N-containing pyrolysis products was small. Feedstock samples showed diketodipyrrole (23) originating from hydroxyproline–hydroxyproline dipeptides in proteins (Chiavari and Galletti, 1992). The proportion increased slightly in the 400 °C biochar, especially in the case of WI-400. Most N products tended to be absent from high temperature biochar, except for benzonitrile (6), which is the dominant pyrolysis product of high temperature char (Kaal et al., 2008b); its origin (e. g. amide, amine or heterocyclic polyaromatic moieties) is unknown (Kaal et al., 2009).

3.4.6. Other compounds

A series of several other groups of minor compounds was detected, but is not reported in Table 4 unless specified. C₁₂–C₁₈ fatty acids (FAs; even numbered only) occurred in all feedstock pyrolysates, with C₁₆ (25) the most abundant (Fig. 2A–C; Table 4). They were not present in the biochar products except for WI-400. Some catechols (catechol – 12, and 4-methylcatechol; Table 4) were detected, which may originate from tannins (Galletti et al., 1995) but also from demethylated lignin (Amen-Chen et al., 2001). The proportion decreased with increasing temperature. A series of triterpenoids occurred in the pyrograms of all feedstock samples; yet they were absent from the biochar pyrolysates. A series of *n*-alkanes/*n*-alkenes was detected in all feedstock types and all biochar samples. In general, the members were of shorter chain length (C₁₀–C₂₀) and were more branched in the pyrolysates of the biochars than in the pyrolysates of the corresponding feedstock (C₁₅–C₃₀). Branching and chain length shortening are well known effects of charring on linear aliphatic C chains (Eckmeier and Wiesenberg, 2009; Wiesenberg et al., 2009). Finally some *n*-alkyl benzenes larger than C₃ alkyl benzene (C₄–C₁₄), which cannot be produced on pyrolysis of lignin, probably originate from cyclisation of linear C chains in combination with artificial charring during pyrolysis (Saiz-Jimenez, 1994).

3.5. Solid state CPMAS ¹³C NMR spectroscopy

The solid state CPMAS ¹³C NMR spectra indicate that the 400 °C biochar (Fig. 3A–C) contained a broader range of C types than the 550 °C biochar (Fig. 3D and E). The PO-400 biochar showed a large peak in the aromatic region at ca. 128 ppm and had a broad band in the alkyl-C region (0–45 ppm); part of the alkyl intensity detected could be due to the presence of spinning side bands (SSBs). The PI-400 and WI-400 biochar spectra also showed a large peak at ca. 128 ppm, along with a peak at ca. 144–147 ppm, assigned to O-substituted aromatic C probably derived from lignin. In the spectra of these two samples, it is likely that the aromatic C is underestimated, as CPMAS ¹³C NMR spectroscopy often under-detects aromatic C and an unequivocal quantification is not feasible (Smernik et al., 2002). These two samples also showed a small peak at ca. 75 ppm (O-alkyl C), which could be attributed to remaining cellulose. The alkyl C area (0–45 ppm) was also evident (Fig. 3A–C).

The spectrum of PI-550 biochar (Fig. 3D) was dominated by a single peak at ca. 128 ppm attributed to C- and H-substituted aromatic C. The next largest peaks in the spectra (marked *) were also related to this peak (as SSBs). The PO-550 spectrum resembled that of PI-550, but showed a small peak at ca. 150 ppm (O/C-aryl C) (Fig. 3E). Finally, the WI-550 biochar had a sharp aromatic peak at ca. 128 ppm and a band in the alkyl-C region was detected (Fig. 3F). Part of the alkyl intensity detected could again be due to the presence of SSBs.

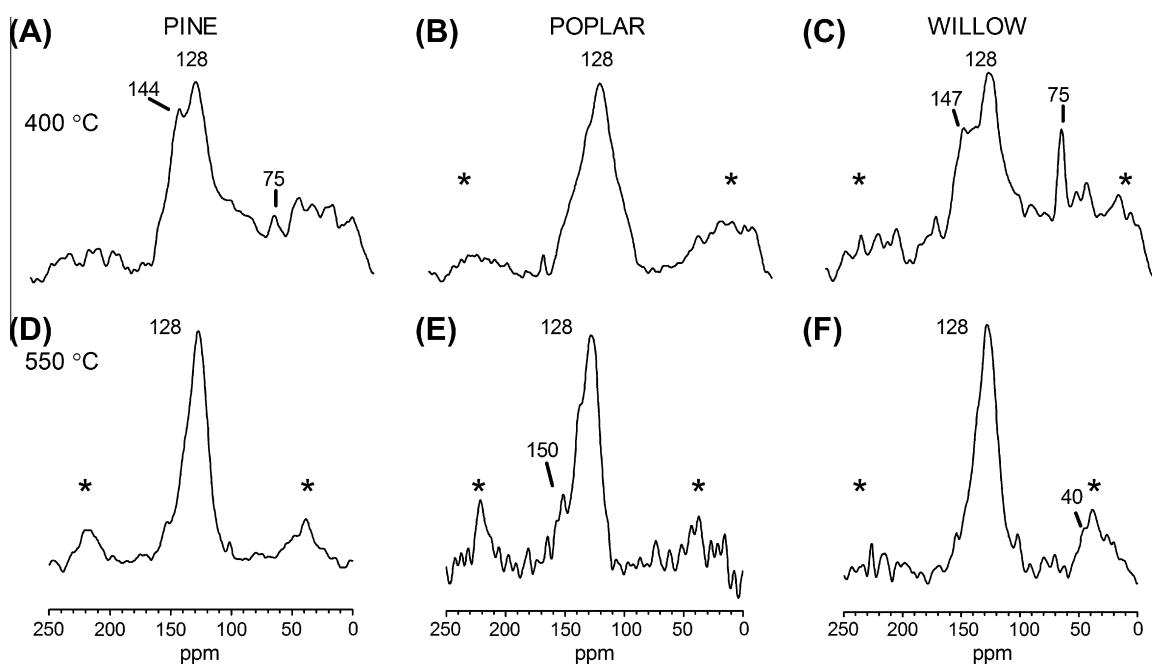


Fig. 3. Solid state ^{13}C NMR spectra of biochar samples (highest heating temperature 400 and 550 °C). (A and D) pine, (B and E) poplar, and (C and F) willow (*, SSBs for aromatic signals).

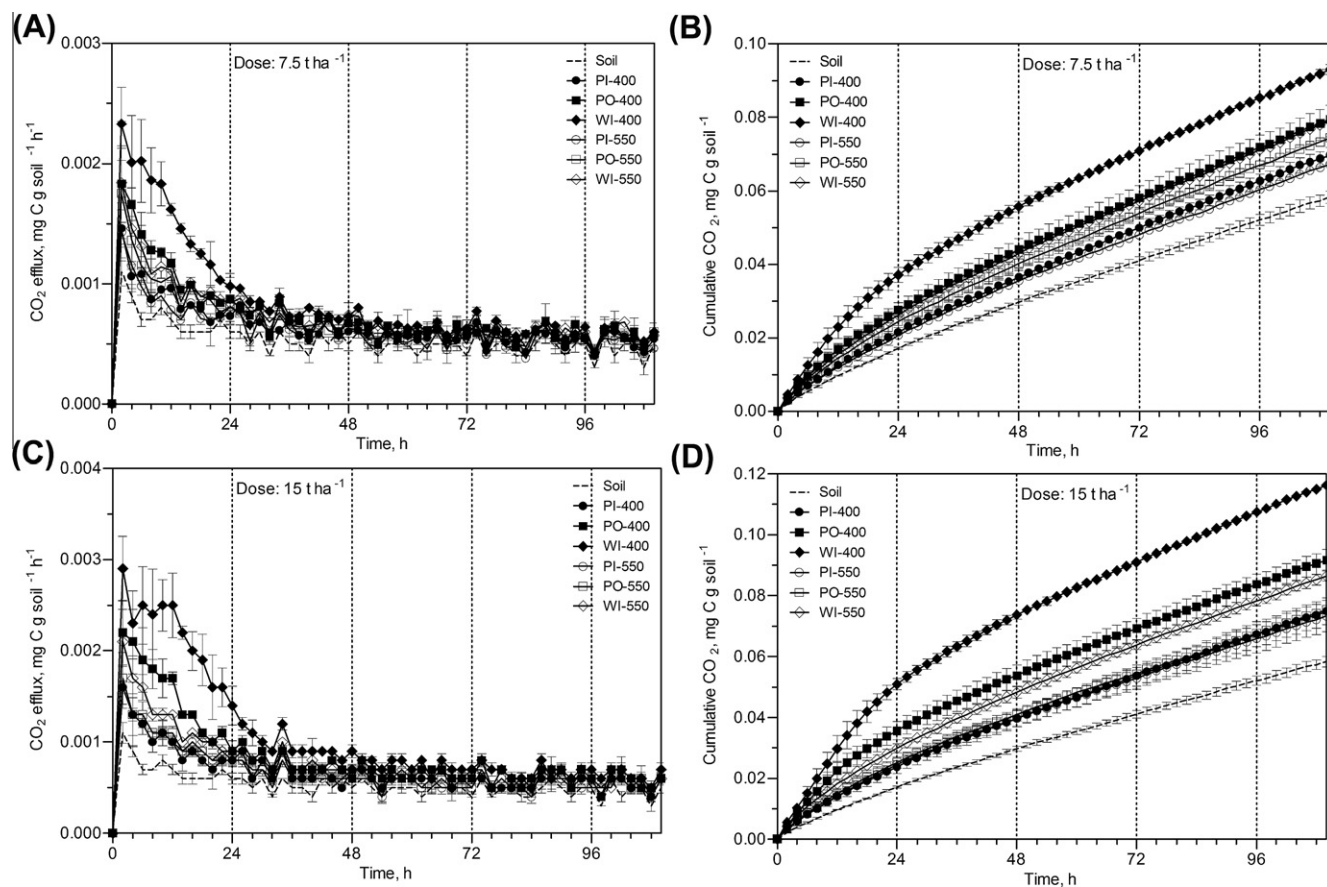


Fig. 4. (A) Amount of $\text{CO}_2\text{-C}$ released per g of soil from the control soil and the soil–biochar mixtures (biochar dose 7.5 t ha^{-1}); (B) cumulative $\text{CO}_2\text{-C}$ released per g of soil from the control soil and the soil–biochar mixtures (biochar dose 7.5 t ha^{-1}); (C) amount of $\text{CO}_2\text{-C}$ released per g of soil from the control soil and the soil–biochar mixtures (biochar dose 15 t ha^{-1}); and (D) cumulative $\text{CO}_2\text{-C}$ released per g of soil from the control soil and the soil–biochar mixtures (biochar dose 15 t ha^{-1}). Bars indicate standard deviation ($n = 3$).

Table 6

Pearson's r correlation coefficients between main variables related to C fractions defined herein.

	C_{thermo}	$C_{\text{dichro}}/C_{\text{total}}$	$C_{\text{per}}/C_{\text{total}}$	H/C	O/C
C_{thermo}	1.000				
$C_{\text{dichro}}/C_{\text{total}}$	0.891 ^a	1.000			
$C_{\text{per}}/C_{\text{total}}$	0.600	0.728	1.000		
H/C	0.497	0.514	0.912 ^a	1.000	
O/C	0.815 ^a	0.948 ^a	0.824 ^a	0.591	1.000

^a Correlation sig. at $P < 0.05$.

3.6. Short term incubation

Evolution patterns of CO_2 emitted from biochar-amended soil during the 110 h incubation period differed, depending on feedstock type and pyrolysis temperature (Fig. 4). After an initial increase in CO_2 evolution, the rate of C emission tended to decrease for all soil–biochar mixtures (Fig. 4). In general, as pyrolysis temperature increased, the amount of CO_2 evolved from the mixtures decreased and the response of the different biochar samples to decomposition became more uniform. The effect was dose-dependent, as expected (Fig. 4). The CO_2 that evolved followed the order WI-400 > PO-400 > WI-550 > PI-400 \approx PO-550 > PI-550 > control, regardless of biochar dose. Unexpectedly, the PI-400 biochar amended soil showed low CO_2 evolution, but values were still above the control (Fig. 4). The pH of the mixtures after incubation was also measured (data not shown). Results showed a general increase in the pH values of soil after the amendment with biochar, especially for the WI-550 biochar–soil mixture; this increase was not observed for the PI-400 biochar–soil mixture.

3.7. Reconciling biochar lability estimates

In order to identify the relationships between the estimates of the intrinsic labile fraction of the biochar C, we used H/C and O/C atomic ratios, C_{thermo} , $C_{\text{dichro}}/C_{\text{total}}$ and $C_{\text{per}}/C_{\text{total}}$ fractions (Tables 2 and 3). The correlation matrix is reported in Table 6. Only r values significant at $P < 0.05$ are described. The scatter diagrams of the

variables with the highest correlation coefficients are displayed in Fig. 5. The $C_{\text{per}}/C_{\text{total}}$ vs. C_{thermo} diagram has also been included (Fig. 5A), in spite of not being significant at $P < 0.05$, because the outlier in the figure is a strong indication of the low $C_{\text{per}}/C_{\text{total}}$ of the WI-550 biochar. The H/C atomic ratio showed a positive significant correlation with oxidised organic $C_{\text{per}}/C_{\text{total}}$ (r 0.91; $P < 0.05$; Fig. 5B). Positive and significant correlations were found between C_{thermo} and the oxidised organic C_{dichro} fraction (r 0.89; $P < 0.05$; Fig. 5C) and between O/C atomic ratio and the same C_{dichro} fraction (r 0.95; $P < 0.05$; Fig. 5D). No attempts were made to relate the CO_2 –C evolved from the biochar-amended soils and the indexes used here, as (i) it was not possible to distinguish the C source and (ii) incubations were considered too short. No clear relationship was found between the fraction of $\text{IC}/C_{\text{total}}$ and the CO_2 evolved from the soil–biochar incubations.

4. Discussion

4.1. Carbonisation of different feedstocks

4.1.1. Pine carbonisation

Thermal decomposition of pine feedstock at 400 °C was incomplete, as inferred from TG and DTG curves, in which the presence of a thermo-degradable fraction below that temperature was observed (Fig. 1). The fact that pyrolysis was halted immediately after the peak temperature was reached did not allow complete thermal decomposition at that temperature. This is supported by Py–GC–MS, which produced amounts of levoglucosan and methoxyphenols (Fig. 2), as well as by the O-substituted aromatics and O-alkyl C peaks in the ^{13}C NMR spectra (Fig. 3), all of which point to the presence of residual lignin and cellulose. Interestingly, retene-like compounds, markers of incomplete coniferous wood combustion (Ramdahl, 1983; Simoneit, 2002; Estrellan and Iino, 2010), were identified in this PI-400 biochar. These compounds are considered persistent, bio-accumulative and toxic (Estrellan and Iino, 2010); however, levels were very low. The microporosity of this biochar was low, in agreement with a low charring temperature (Keiluweit et al., 2010) and the presence of lignin remnants (Sharma et al., 2004).

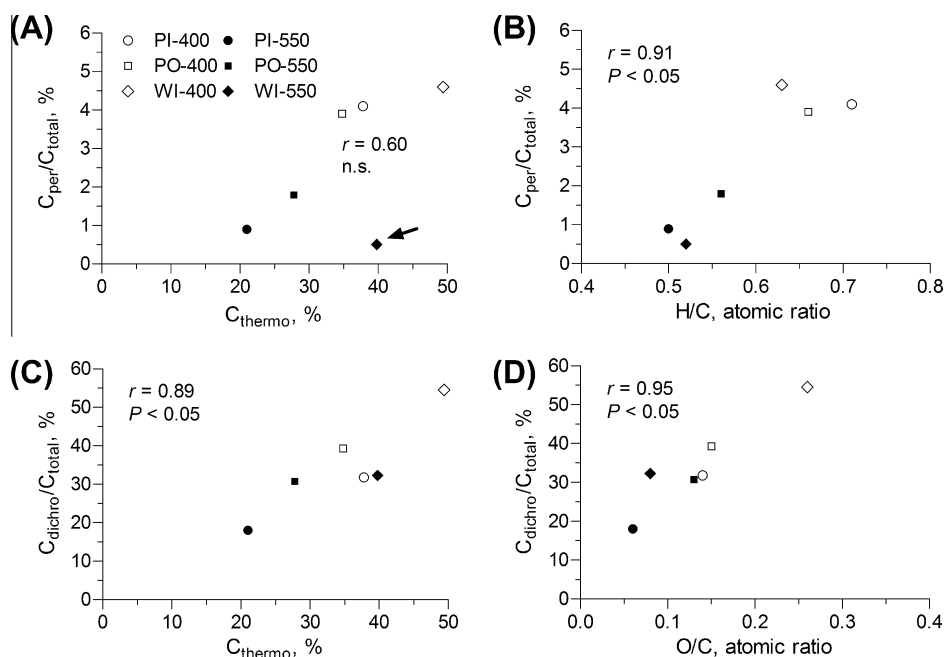


Fig. 5. Correlations between different estimates of biochar lability (C_{thermo} , $C_{\text{per}}/C_{\text{total}}$, $C_{\text{dichro}}/C_{\text{total}}$, H/C atomic ratio, O/C atomic ratio).

Pine pyrolysed at 550 °C underwent more complete carbonisation, as inferred from the decrease in H/C (Hammes et al., 2008). Besides, the TG and DTG curves showed a lack of a thermo-degradable fraction below 550 °C (Fig. 1), whereas the Py–GC–MS pyrogram produced a limited number of peaks, primarily markers of strongly charred biomass (benzene, PAHs, benzonitrile, dibenzofuran); the ^{13}C NMR spectrum was in agreement with these findings. The observed increase in benzene/toluene and naphthalene/ C_1 naphthalene as the pyrolysis temperature increased can be attributed to loss of short chain alkyl cross-linkages (Kaal and Rumpel, 2009). The low heating rate (24 °C min^{-1}) may have had a key role in the high aromaticity and porosity of this sample, facilitating the removal of the volatile fraction from the pore system and increasing the BET surface area. Brown et al. (2006) found similar surface area ($210\text{--}370\text{ m}^2\text{ g}^{-1}$) in pine biochar produced at 525 and 600 °C respectively, under heating rates $<20\text{ °C min}^{-1}$.

4.1.2. Poplar carbonisation

Pyrolysis of poplar at 400 °C produced a relatively thoroughly carbonised biochar, compared with PI-400 (and also WI-400 biochar, as discussed below). This was reflected in (i) a low H/C value; (ii) the virtual absence of a thermo-degradable fraction below that temperature (Fig. 1); (iii) the almost complete disappearance of methoxyphenols and levoglucosan from the pyrolysates (Fig. 2); (iv) the large aryl-C peak in the ^{13}C NMR spectra (Fig. 3). This could be explained by the fact that the biomass was relatively young (1 yr plantation) and/or by the relatively low heating rate at which this biochar was produced (36 °C min^{-1}) compared with other samples (WI-400, 62 °C min^{-1} , PO-550, 48 °C min^{-1}), favouring relatively efficient carbonisation.

Increasing the pyrolysis temperature to 550 °C produced a more aromatic biochar with higher specific surface area than the PO-400 biochar, although some non-aromatic C fractions could still be detected via ^{13}C NMR and Py–GC–MS. Also, the TG and DTG curves showed the presence of non-thermally degraded material at temperatures below 550 °C (incomplete carbonisation). The fast mean heating rate during production of PO-550 (48 °C min^{-1}) could explain this finding. The mentioned “double peaks” for benzene and toluene for the PO-550 biochar (also the WI-550 biochar) might suggest that a considerable quantity of volatiles was trapped in these biochar samples.

4.1.3. Willow carbonisation

The TG and DTG curves of WI-400 provided evidence that a considerable fraction of the charcoal was still degradable at 400 °C, again pointing towards incomplete carbonisation. In addition, the mean heating rate (62 °C min^{-1}) had influenced the poor carbonisation degree. This is consistent with the presence of large peaks for levoglucosan and methoxyphenols (Py–GC–MS) and the presence of O-aryl and O-alkyl C (^{13}C NMR), all indicative of residual or transformed lignin and cellulose. This was corroborated by the high C_{thermo} value for this biochar. Finally, increasing the temperature to 550 °C produced a more aromatic biochar (WI-550) with characteristics similar to PO-550.

4.1.4. Assessment of carbonisation of wood biomass

In short, the techniques provided detailed and consistent information concerning the chemical characterisation of both feedstock and biochar samples. The degree of carbonisation, based mainly on the characterisation of the samples using Py–GC–MS and CPMAS ^{13}C -NMR, increased in the order WI-400 < PI-400 ~ WI-550 ~ PO-400 < PO-550 < PI-550; this was corroborated by the elemental analysis and TG results. It can also be inferred from the results that, for a more complete carbonisation of the feedstock, it is not only feedstock type and final pyrolysis temperature that are important, but also the heating rate. To ensure the complete release of vola-

tiles, holding the peak temperature at the end of the pyrolysis process (Sutcu, 2007; Ertas and Hakki Alma, 2010) is recommended. A drop in temperature below the boiling point of the product before the gas had time to move out of the biochar along the exhaust may have resulted in products trapped in the biochar. An adequate adjustment of these conditions will be crucial in large biochar production operations.

4.2. CO_2 evolved from biochar–soil incubation

The addition of biochar to the soil enhanced CO_2 evolution vs. the control. Low temperature biochar (except PI-400) induced a higher CO_2 efflux than high temperature biochar. These results match well with the structural biochemical properties deduced from the spectroscopic techniques and were corroborated by the TG and DTG curves, suggesting that the response on CO_2 efflux can to some extent be related to the intrinsic labile C fraction of added biochar. However, a minor contribution of carbonate to the CO_2 released from soils amended with WI-400, PO-550 and WI-550 biochar samples should not be discounted, as the ash in the biochar would tend to dissolve in the acidic environment of this soil. Unexpectedly, PI-400 followed a pattern similar to that of high temperature biochar samples. Several factors could have caused this behaviour: (i) its relatively limited liming ability; (ii) the absence of carbonate; (iii) a very low surface area; and/or (iv) the presence of substances potentially toxic to soil microflora (e.g. diterpenoids and their derivatives). It is worth noting that the $\text{C}_{\text{dichro}}/\text{C}_{\text{total}}$ value of the PI-400 biochar was smaller than would be expected on the basis of thermo-labile C content (TG data, C_{thermo} ; Table 3). This might suggest that the $\text{C}_{\text{dichro}}/\text{C}_{\text{total}}$ index better reflects the short term behaviour of biochar in soil than do TG techniques.

Overall, the findings confirm the important role of the degree of thermal alteration on the short term evolution of CO_2 from biochar–soil mixtures (Baldock and Smernik, 2002; Bruun et al., 2008, 2011; Zimmerman et al., 2011). In addition to C lability in biochar, other factors reported to promote CO_2 evolution from biochar-amended soil include: (i) internal microporosity (Nguyen et al., 2004; Hammes et al., 2008), (ii) the presence of carbonate in the ash (Bruun et al., 2008), (iii) the presence of nutrients in the ash (Nguyen et al., 2010) and/or (iv) abiotic oxidation of fresh biochar (Cheng et al., 2006).

4.3. Assessment of labile fraction of biochar–C

The intrinsic lability of the different biochar samples, as revealed from the spectroscopic methods, was consistently reflected in the thermogravimetric analysis and therefore in the C_{thermo} data, resulting in a trend in thermo-lability: WI-400 > PI-400 ~ WI-550 ~ PO-400 > PO-550 > PI-550. The other indices (H/C, O/C, $\text{C}_{\text{per}}/\text{C}_{\text{total}}$ and $\text{C}_{\text{dichro}}/\text{C}_{\text{total}}$) showed, in general, a similar order (Table 3). Values of C_{thermo} and $\text{C}_{\text{dichro}}/\text{C}_{\text{total}}$ had the same order of magnitude, but this was not the case for $\text{C}_{\text{per}}/\text{C}_{\text{total}}$ values, which were 20 times lower on average, as alkaline permanganate was unable to oxidise a considerable extent of organic C in the biochar (<5% of C_{total}). In general, results indicate that TG and wet oxidation with potassium dichromate reflected the degree of wood biomass carbonisation and could therefore be used to estimate the labile fraction of C in biochar.

The use of an oxidation reagent, such as potassium dichromate and potassium permanganate, for the determination of the labile fraction of C in biochar assumes that the reagent does not react with the aromatic C structure of charcoal, which is not always the case (Knicker et al., 2007, 2008). The use of potassium dichromate for the quantification of BC has been questioned on the basis of the observed oxidation of aromatic C – with a concurrent

underestimate of the charred fraction of C – and also on the lack of reactivity of an acid-resistant alkyl fraction – with a resulting overestimate of the charred fraction of C (Knicker et al., 2007, 2008). However, a similar oxidation method has been used for isolating highly aromatic BC-type materials, either fresh or protected from extensive degradation (Krull et al., 2006).

Further efforts are needed to characterise the fraction of biochar after wet oxidation and to study the kinetics of the reactions, as carried out earlier for soils, sediments, or kerogen (Wolbach and Anders, 1989; Knicker et al., 2007). Additional factors that must be considered when using these methodologies are particle size, microstructure and reactive surface area (Wolbach and Anders, 1989; Hammes et al., 2008; Nocentini et al., 2010).

5. Conclusions

The influence of feedstock type and pyrolysis conditions on the degree of carbonisation and other biochar properties was evidenced via solid state ^{13}C NMR and Py–GC–MS. Characterisation was paralleled by the application of low cost analytical techniques (e.g. TG, wet oxidation), providing qualitative and quantitative information that was used to assess the intrinsic lability of C in biochar. The results can imply that dichromate oxidation and TG could be used to estimate the intrinsic labile fraction of C in biochar. However, a wider range of biochar type and long term field studies are needed before any technique to be used in routine analysis can be recommended for assessing biochar lability in soil. Special attention will need to be paid to the potential influence of the mineral fraction (e.g. liming ability, carbonate and nutrient content) and the presence of volatile organic compounds that may inhibit microbial activity. Specific absolute values of the labile fraction of C in biochar are also needed if biochar is to be accounted for in C trading schemes.

Acknowledgments

The authors acknowledge financial support from the Ministry of Agriculture and Forestry of New Zealand. They would like to thank the staff of the Departamento Edafología y Química Agrícola, USC – Campus de Lugo, for the pressure plate measurements, and F. Jackson (Nutrition Laboratory, Massey University) for cellulose, hemicellulose and lignin content determination. R.C.P. was partly funded by the NZAGRC. J.A.M.-A. thanks the Spanish MCyT via the award of a Juan de la Cierva contract. The authors are grateful to M. Bretherton and P. Bishop for technical support, timely guidance and useful comments, and thank E.S. Krull and an anonymous reviewer for helpful comments and suggestions.

Associate Editor—S. Derenne

References

Ahmedna, M., Johns, M.M., Clarke, S.J., Marshall, W.E., Rao, R.M., 1997. Potential of agricultural by-product-based activated carbons for use in raw sugar decolourisation. *Journal of the Science of Food and Agriculture* 75, 117–124.

Amen-Chen, C., Pakdel, H., Roy, C., 2001. Production of monomeric phenols by thermochemical conversion of biomass: a review. *Bioresource Technology* 79, 277–299.

Baldock, J.A., Smernik, R.J., 2002. Chemical composition and bioavailability of thermally altered *Pinus resinosa* (Red pine) wood. *Organic Geochemistry* 33, 1093–1109.

Boon, J.J., Pastorova, I., Botto, R.E., Arisz, P.W., 1994. Structural studies on cellulose pyrolysis and cellulose chars by PYMS, PYGCMS, FTIR, NMR and by wet chemical techniques. *Biomass and Bioenergy* 7, 25–32.

Brodowski, S., Rodionov, A., Haumaier, L., Glaser, B., Amelung, W., 2005. Revised black carbon assessment using benzene polycarboxylic acids. *Organic Geochemistry* 36, 1299–1310.

Brown, R.A., Kercher, A.K., Nguyen, T.H., Nagle, D.C., Ball, W.P., 2006. Production and characterization of synthetic wood char for use as surrogates for natural sorbents. *Organic Geochemistry* 37, 321–333.

Brunauer, S., Emmett, P.H., Teller, E., 1938. Adsorption of gases in multimolecular layers. *Journal of the American Chemical Society* 60, 309–319.

Bruun, S., Jensen, E.S., Jensen, L.S., 2008. Microbial mineralization and assimilation of black carbon: dependency on degree of thermal alteration. *Organic Geochemistry* 39, 839–845.

Bruun, E.W., Hauggaard-Nielsen, H., Ibrahim, N., Egsgaard, H., Ambus, P., Jensen, P.A., Dam-Johansen, K., 2011. Influence of fast pyrolysis temperature on biochar labile fraction and short-term carbon loss in a loamy soil. *Biomass and Bioenergy* 35, 1182–1189.

Cheng, C.-H., Lehmann, J., Thies, J.E., Burton, S.D., Engelhard, M.H., 2006. Oxidation of black carbon by biotic and abiotic processes. *Organic Geochemistry* 37, 1477–1488.

Chiavari, G., Galletti, G.C., 1992. Pyrolysis–gas chromatography/mass spectrometry of amino acids. *Journal of Analytical and Applied Pyrolysis* 24, 123–137.

Czimczik, C.I., Masiello, C.A., 2007. Controls on black carbon storage in soils. *Global Biogeochemistry Cycles* 21, GB3005.

de la Rosa, J.M., Knicker, H., López-Capel, E., Manning, D.A.C., González-Perez, J.A., González-Vila, F.J., 2008. Direct detection of black carbon in soils by Py–GC/MS, ^{13}C NMR spectroscopy and thermogravimetric techniques. *Soil Science Society of America Journal* 72, 258–267.

Eckmeier, E., Wiesenberg, G.L.B., 2009. Short-chain *n*-alkanes (C_{16-20}) in ancient soil are useful molecular markers for prehistoric biomass burning. *Journal of Archaeological Science* 36, 1590–1596.

Ertas, M., Hakki Alma, M., 2010. Pyrolysis of laurel (*Laurus nobilis* L.) extraction residues in a fixed-bed reactor: characterization of bio-oil and bio-char. *Journal of Analytical and Applied Pyrolysis* 88, 22–29.

Estrellan, C.R., Iino, F., 2010. Toxic emissions from open burning. *Chemosphere* 80, 193–207.

Faix, O., Meier, D., Grobe, I., 1987. Studies on isolated lignins and lignins in woody materials by pyrolysis–gas chromatography–mass spectrometry and off-line pyrolysis–gas chromatography with flame ionization detection. *Journal of Analytical and Applied Pyrolysis* 11, 403–416.

Forster, P., Artaxo, P., Betts, R., Fahey, D.W., Haywood, J., Lean, J., Lowe, D.C., Myhre, G., Nganga, J., Prinn, R., Raga, G., Schulz, M., Van Dorland, R., 2007. Changes in atmospheric constituents and in radiative forcing. In: Solomon, S., Qin, D., Manning, M., Chen, Z., Marquis, M., Averyt, K., Tignor, M., Miller, H. (Eds.), *Climate Change 2007: The Physical Science Basis. Contribution of Working Group I to the Fourth Assessment Report of the Intergovernmental Panel on Climate Change*. Cambridge University Press, Cambridge, United Kingdom and New York, NY, USA, pp. 129–234.

Galletti, G.C., Modafferi, V., Poiana, M., Bocchini, P., 1995. Analytical pyrolysis and thermally assisted hydrolysis–methylation of wine tannin. *Journal of Agricultural and Food Chemistry* 43, 1859–1863.

Hammes, K., Schmidt, M.W.I., 2009. Changes in biochar in soil. In: Lehmann, J., Joseph, S. (Eds.), *Biochar for Environmental Management. Science and Technology*. Earthscan, London, pp. 169–181.

Hammes, K., Schmidt, M.W.I., Smernik, R.J., Currie, L.A., Ball, W.P., Nguyen, T.H., Louchouart, P., Houel, S., Gustafsson, Ö., Elmquist, M., Cornelissen, G., Skjemstad, J.O., Masiello, C.A., Song, J., Peng, P.a., Mitra, S., Dunn, J.C., Hatcher, P.G., Hockaday, W.C., Smith, D.M., Hartkopf-Fröder, C., Böhmer, A., Lühr, B., Huebert, B.J., Amelung, W., Brodowski, S., Huang, L., Zhang, W., Gschwend, P.M., Flores-Cervantes, D.X., Largeau, C., Rouzaud, J.-N., Rumpel, C., Guggenberger, G., Kaiser, K., Rodionov, A., Gonzalez-Vila, F.J., Gonzalez-Perez, J.A., de la Rosa, J.M., Manning, D.A.C., López-Capel, E., Ding, L., 2007. Comparison of quantification methods to measure fire-derived (black/elemental) carbon in soils and sediments using reference materials from soil, water, sediment and the atmosphere. *Global Biogeochemistry Cycles* 21, GB3016.

Hammes, K., Smernik, R.J., Skjemstad, J.O., Schmidt, M.W.I., 2008. Characterisation and evaluation of reference materials for black carbon analysis using elemental composition, colour, BET surface area and ^{13}C NMR spectroscopy. *Applied Geochemistry* 23, 2113–2122.

Hina, K., Bishop, P., Arbestain, M.C., Calvelo-Pereira, R., Maciá-Agulló, J.A., Hindmarsh, J., Hanly, J.A., Macías, F., Hedley, M.J., 2010. Producing biochars with enhanced surface activity through alkaline pretreatment of feedstocks. *Australian Journal of Soil Research* 48, 606–617.

Kaal, J., Rumpel, C., 2009. Can pyrolysis–GC/MS be used to estimate the degree of thermal alteration of black carbon? *Organic Geochemistry* 40, 1179–1187.

Kaal, J., Brodowski, S., Baldock, J.A., Nierop, K.G.J., Martínez Cortizas, A., 2008a. Characterisation of aged black carbon using pyrolysis–GC/MS, thermally assisted hydrolysis and methylation (THM), direct and cross-polarisation ^{13}C nuclear magnetic resonance (DP/CP NMR) and the benzene polycarboxylic acid (BPCA) method. *Organic Geochemistry* 39, 1415–1426.

Kaal, J., Martínez-Cortizas, A., Nierop, K.G.J., Buurman, P., 2008b. A detailed pyrolysis–GC/MS analysis of a black carbon-rich acidic colluvial soil (Atlantic ranker) from NW Spain. *Applied Geochemistry* 23, 2395–2405.

Kaal, J., Martínez Cortizas, A., Nierop, K.G.J., 2009. Characterisation of aged charcoal using a coil probe pyrolysis–GC/MS method optimised for black carbon. *Journal of Analytical and Applied Pyrolysis* 85, 408–416.

Keiluweit, M., Nico, P.S., Johnson, M.G., Kleber, M., 2010. Dynamic molecular structure of plant biomass-derived black carbon (biochar). *Environmental Science and Technology* 44, 1247–1253.

Kimetu, J.M., Lehmann, J., 2010. Stability and stabilisation of biochar and green manure in soil with different organic carbon contents. *Australian Journal of Soil Research* 48, 577–585.

- Knicker, H., Müller, P., Hilscher, A., 2007. How useful is chemical oxidation with dichromate for the determination of "black carbon" in fire-affected soils? *Geoderma* 142, 178–196.
- Knicker, H., Hilscher, A., González-Vila, F.J., Almendros, G., 2008. A new conceptual model for the structural properties of char produced during vegetation fires. *Organic Geochemistry* 39, 935–939.
- Krull, E.S., Swanston, C.W., Skjemstad, J.O., McGowan, J.A., 2006. Importance of charcoal in determining the age and chemistry of organic carbon in surface soils. *Journal of Geophysical Research* 111, G04001.
- Kuzyakov, Y., Subbotina, I., Chen, H., Bogomolova, I., Xu, X., 2009. Black carbon decomposition and incorporation into soil microbial biomass estimated by ^{14}C labeling. *Soil Biology and Biochemistry* 41, 210–219.
- Labbe, N., Harper, D., Rials, T., Elder, T., 2006. Chemical structure of wood charcoal by infrared spectroscopy and multivariate analysis. *Journal of Agricultural and Food Chemistry* 54, 3492–3497.
- Lehmann, J., Joseph, S., 2009. Biochar for Environmental Management. Science and Technology. Earthscan, London.
- Lehmann, J., Gaunt, J., Rondon, M., 2006. Bio-char sequestration in terrestrial ecosystems – a review. *Mitigation and Adaptation Strategies for Global Change* 11, 395–419.
- Lehmann, J., Czimczik, C., Laird, D., Sohi, S., 2009. Stability of biochar in soil. In: Lehmann, J., Joseph, S. (Eds.), *Biochar for Environmental Management. Science and Technology*. Earthscan, London, pp. 183–205.
- Macías, F., Camps Arbustain, M., 2010. Soil carbon sequestration in a changing global environment. *Mitigation and Adaptation Strategies for Global Change* 15, 511–529.
- Marques Trompowsky, P., Benites, V.D.M., Madari, B.E., Pimenta, A.S., Hockaday, W.C., Hatcher, P.G., 2005. Characterization of humic like substances obtained by chemical oxidation of eucalyptus charcoal. *Organic Geochemistry* 36, 1480–1489.
- McBeath, A.V., Smernik, R.J., 2009. Variation in the degree of aromatic condensation of chars. *Organic Geochemistry* 40, 1161–1168.
- Michel, K., Terhoeven-Urselmans, T., Nitschke, R., Steffan, P., Ludwig, B., 2009. Use of near- and mid-infrared spectroscopy to distinguish carbon and nitrogen originating from char and forest-floor material in soils. *Journal of Plant Nutrition and Soil Science* 172, 63–70.
- Nguyen, B.T., Lehmann, J., 2009. Black carbon decomposition under varying water regimes. *Organic Geochemistry* 40, 846–853.
- Nguyen, T.H., Brown, R.A., Ball, W.P., 2004. An evaluation of thermal resistance as a measure of black carbon content in diesel soot, wood char, and sediment. *Organic Geochemistry* 35, 217–234.
- Nguyen, B.T., Lehmann, J., Hockaday, W.C., Joseph, S., Masiello, C.A., 2010. Temperature sensitivity of black carbon decomposition and oxidation. *Environmental Science and Technology* 44, 3324–3331.
- Nocentini, C., Certini, G., Knicker, H., Francioso, O., Rumpel, C., 2010. Nature and reactivity of charcoal produced and added to soil during wildfire are particle-size dependent. *Organic Geochemistry* 41, 682–689.
- Paris, O., Zollfrank, C., Zickler, G.A., 2005. Decomposition and carbonisation of wood biopolymers – a microstructural study of softwood pyrolysis. *Carbon* 43, 53–66.
- Pastorova, I., Botto, R.E., Arisz, P.W., Boon, J.J., 1994. Cellulose char structure: a combined analytical Py–GC–MS, FTIR, and NMR study. *Carbohydrate Research* 262, 27–47.
- Pouwels, A.D., Eijkel, G.B., Boon, J.J., 1989. Curie-point pyrolysis–capillary gas chromatography–high-resolution mass spectrometry of microcrystalline cellulose. *Journal of Analytical and Applied Pyrolysis* 14, 237–280.
- Ramdahl, T., 1983. Retene – a molecular marker of wood combustion in ambient air. *Nature* 306, 580–582.
- Robertson, J.B., Van Soest, P.J., 1981. The detergent system of analysis and its application to human foods. In: James, W.P.T., Theander, O. (Eds.), *The Analysis of Dietary Fiber in Food*. Marcel Dekker, Inc., New York, 123pp.
- Rumpel, C., González-Pérez, J.A., Bardoux, G., Largeau, C., Gonzalez-Vila, F.J., Valentin, C., 2007. Composition and reactivity of morphologically distinct charred materials left after slash-and-burn practices in agricultural tropical soils. *Organic Geochemistry* 38, 911–920.
- Saiz-Jimenez, C., 1994. Production of alkylbenzenes and alkylnaphthalenes upon pyrolysis of unsaturated fatty acids. *Naturwissenschaften* 81, 451–453.
- Schnitzer, M.I., Monreal, C.M., Jandl, G., Leinweber, P., Fransham, P.B., 2007. The conversion of chicken manure to biooil by fast pyrolysis II. Analysis of chicken manure, biooils, and char by curie-point pyrolysis–gas chromatography/mass spectrometry (Cp Py–GC/MS). *Journal of Environmental Science and Health, Part B: Pesticides, Food Contaminants, and Agricultural Wastes* 42, 79–95.
- Sevilla, M., Fuertes, A.B., 2010. Graphitic carbon nanostructures from cellulose. *Chemical Physics Letters* 490, 63–68.
- Shackley, S., Sohi, S., 2010. An Assessment of the Benefits and Issues Associated with the Application of Biochar to Soil. UK Biochar Research Centre, Edinburgh, UK, 132pp.
- Sharma, R.K., Wooten, J.B., Baliga, V.L., Lin, X., Geoffrey Chan, W., Hajaligol, M.R., 2004. Characterization of chars from pyrolysis of lignin. *Fuel* 83, 1469–1482.
- Simoneit, B.R.T., 2002. Biomass burning – a review of organic tracers for smoke from incomplete combustion. *Applied Geochemistry* 17, 129–162.
- Smernik, R.J., Baldock, J.A., Oades, J.M., 2002. Impact of remote protonation on ^{13}C CPMAS NMR quantitation of charred and uncharred wood. *Solid State Nuclear Magnetic Resonance* 22, 71–82.
- Song, J., Peng, P., 2010. Characterisation of black carbon materials by pyrolysis–gas chromatography–mass spectrometry. *Journal of Analytical and Applied Pyrolysis* 87, 129–137.
- Sutcu, H., 2007. Pyrolysis of peat: product yield and characterization. *Korean Journal of Chemical Engineering* 24, 736–741.
- Tirol-Padre, A., Ladha, J.K., 2004. Assessing the reliability of permanganate-oxidizable carbon as an index of soil labile carbon. *Soil Science Society of America Journal* 68, 969–978.
- Vassileva, C.G., Vassilev, S.V., 2005. Behaviour of inorganic matter during heating of Bulgarian coals: 1. Lignites. *Fuel Processing Technology* 86, 1297–1333.
- Verheijen, F.G.A., Jeffery, S., Bastos, A.C., van der Velde, M., Diafas, I., 2009. Biochar Application to Soils – A Critical Scientific Review of Effects on Soil properties, Processes and Functions. EUR 24099 EN. Office for the Official Publications of the European Communities, Luxembourg, 149pp.
- Wiesenberg, G.L.B., Lehndorff, E., Schwark, L., 2009. Thermal degradation of rye and maize straw: lipid pattern changes as a function of temperature. *Organic Geochemistry* 40, 167–174.
- Wolbach, W.S., Anders, E., 1989. Elemental carbon in sediments: determination and isotopic analysis in the presence of kerogen. *Geochimica et Cosmochimica Acta* 53, 1637–1647.
- Zimmerman, A.R., 2010. Abiotic and microbial oxidation of laboratory-produced black carbon (biochar). *Environmental Science and Technology* 44, 1295–1301.
- Zimmerman, A.R., Gao, B., Ahn, M.-Y., 2011. Positive and negative carbon mineralization priming effects among a variety of biochar-amended soils. *Soil Biology and Biochemistry* 43, 1169–1179.